

3D Magnetic Resonance Fingerprinting with a Clustered Spatiotemporal Dictionary

Pedro A Gómez^{1,2}, Guido Bounincontri³, Miguel Molina-Romero^{1,2},
Cagdas Ulas^{1,2}, Jonathan I Sperl², Marion I Menzel², Bjoern H Menze¹

¹Computer Science, Technische Universität München, Munich, Germany

²GE Global Research, Munich, Germany

³INFN Pisa, Pisa, Italy

Abstract. We present a method for creating a spatiotemporal dictionary for magnetic resonance fingerprinting (MRF). Our technique is based on the clustering of multi-parametric spatial kernels from training data and the posterior simulation of a temporal fingerprint for each voxel in every cluster. We show that the parametric maps estimated with a clustered dictionary agree with maps estimated with a full dictionary, and are also robust to undersampling and shorter sequences, leading to increased efficiency in parameter mapping with MRF.

1 Purpose

Magnetic resonance fingerprinting (MRF) allows for the simultaneous quantification of multiple tissue properties via the matching of acquired signals to a pre-computed dictionary, created by sampling a wide range of the parameter space [4]. As the parameters of interest increase, so does the dictionary size, leading to long reconstruction times. One possibility for overcoming this limitation is to use a clustered dictionary with both spatial and temporal information [2]. This work aims at increasing MRF efficiency by using a clustered spatiotemporal dictionary and incorporating it into a MRF pipeline that includes B1 mapping and a view-sharing (VS) anti-aliasing strategy [1].

2 Methods

We tested our approach using 3D MRF data of a Lister-hooded adult rat brain adult acquired with a Bruker BioSpec 47/40 system (Bruker Inc., Ettlingen, Germany) [1]. The sequence was based on SSFP-MRF [3] with Cartesian sampling, $T = 1000$ shots, and 0.5 mm isotropic resolution. A dictionary $\mathbf{D} \in \mathbb{C}^{L \times T}$ was simulated using extended phase graphs with the following ranges: T1 from 100ms to 3,000ms in 20ms steps; T2 from 20ms to 100ms in 5ms steps and from 100 to 500ms in 10ms steps; and B1 as a flip angle factor from 50% to 150% in 1% steps, resulting in a dictionary of size 840522×1000 . The acquired data was matched to the dictionary to create a reference dataset.

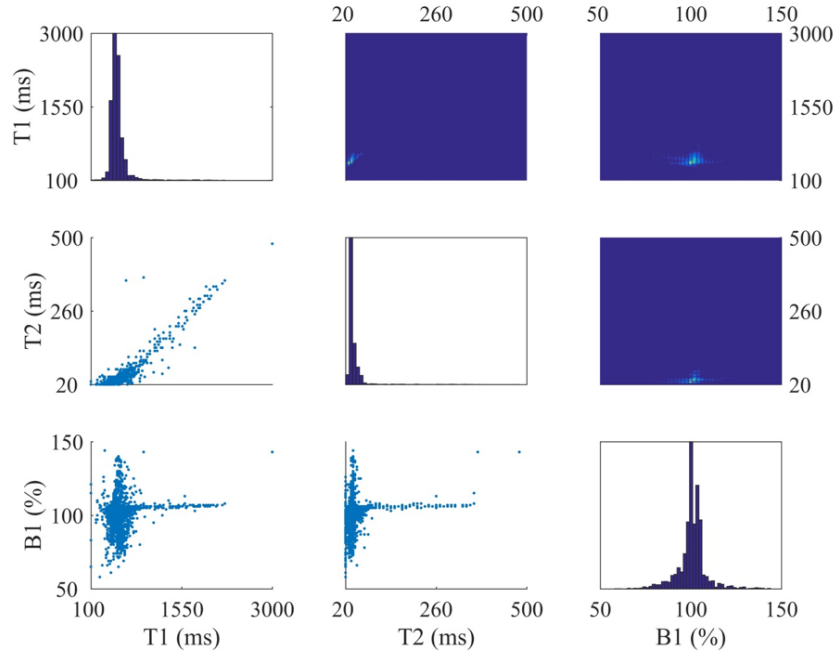


Fig. 1. Parameter distribution obtained from selected slices in the left hemisphere used as a training dataset. The upper triangle displays density plots, the diagonal histograms, and the lower triangle scatter plots. Note that parameters approach a Gaussian distribution and are densely scattered within a specific range.

Exploiting symmetry of the brain, the reference dataset was divided along the medial longitudinal fissure, separating the left and right hemisphere. The estimated parametric T1, T2 and B1 maps of the left hemisphere (see Fig. 1) were used to create spatiotemporal dictionaries of different sizes by first clustering multi-parametric (T1, T2, B1) spatial kernels using k-means and subsequently simulating the temporal signal of every voxel in each cluster. The right hemisphere of the reference dataset was then matched to dictionaries with spatial kernel sizes of $P = 1 \times 1 \times 1$ (clustered only), $P = 3 \times 3 \times 3$ and $P = 5 \times 5 \times 5$ (see Fig. 2).

We hypothesize that a dictionary that contains only feasible parameter combinations and spatial information should enable acceleration in both space and time. We test this by samplingless k-space points using a Gaussian mask in the phase encode directions with different acceleration factors (Figs. 3-4), and by reducing the sequence length (Fig. 4). Undersampled datasets were reconstructed with the original dictionary template matching (TM) [4] and with our VS approach, and compared to the reference dataset by their similarity index (SSIM) [5]. Furthermore, we study the amount of clusters required to accurately capture the entire spatio-parametric variability in our dataset by evaluating the mean

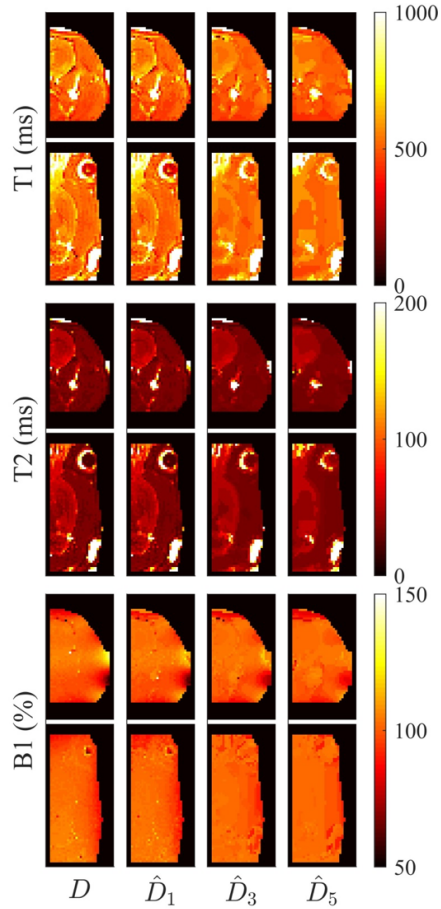


Fig. 2. Comparison of the estimated T1, T2 and B1 parametric maps from the fully sampled dataset with a temporal dictionary $\mathbf{D} \in \mathbb{C}^{L \times T}$ and three clustered dictionaries $\hat{\mathbf{D}}_{\sqrt[3]{P}} \in \mathbb{C}^{K \times T \times P}$ with $K = 300$, $T = 1000$, and $P = 1 \times 1 \times 1$, $3 \times 3 \times 3$, and $5 \times 5 \times 5$. Spatial smoothing obtained with and is achieved by averaging all contributing patches to a given voxel.

square error (MSE) of the training and testing data for different spatial kernels (Fig. 5).

3 Results

Figure 1 shows how the estimated parameters approximate a Gaussian distribution, and are scattered in a restricted range within the parameter space. Hence, using dictionaries trained from this distribution yields parametric maps that agree with maps estimated using the full dictionary (see Fig. 2). Figure 3 com-

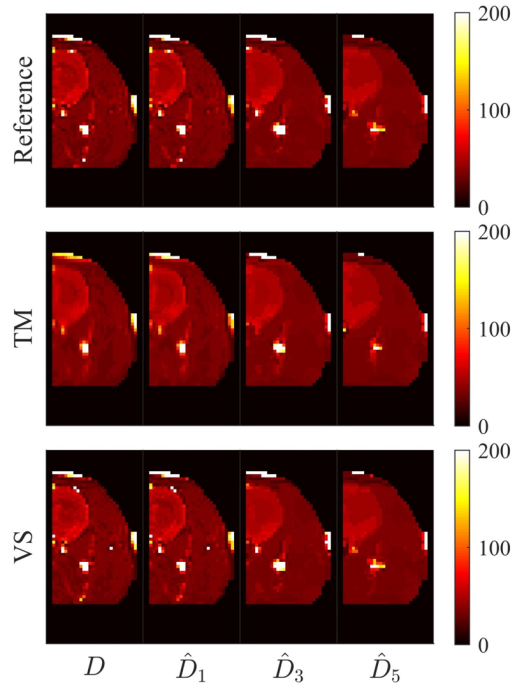


Fig. 3. Estimated T2 parametric maps from fully sampled reference data and data undersampled with an acceleration factor $R=5$ (20% of k-space) for two different reconstruction methods: template matching (TM) and view-sharing (VS). The clustered dictionaries $\hat{\mathbf{D}}_{\sqrt[3]{P}} \in \mathbb{C}^{K \times T \times P}$ consisted of $K = 300$, $T = 1000$, and $P = 1 \times 1 \times 1$, $3 \times 3 \times 3$, and $5 \times 5 \times 5$.

compares the reconstructed maps with 20% sampling of k-space, where \mathbf{D} and $\hat{\mathbf{D}}_1$ combined with VS are the most similar to the reference dataset. Figure 4 shows smaller variation of the clustered dictionaries with undersampling, though having less similarity to the reference dataset in fully sampled cases. Fig. 5 evidences how the training error decreases for more clusters in all cases, while the testing error only decreases continuously for $\hat{\mathbf{D}}_1$.

4 Discussion

We use spatiotemporal dictionaries of different spatial kernel sizes with $K = 300$ clusters (0.036% of the original dictionary size) and obtain comparable parametric maps (see Fig. 2). Furthermore, Figs. 3-4 show that clustered dictionaries, especially if they contain spatial information, are more robust to undersampling and shorter sequences. Conversely, the spatial smoothing achieved with larger spatial kernels along with the constant testing errors for increasing clusters in Fig. 5 indicate that the training data does not accurately represent the testing

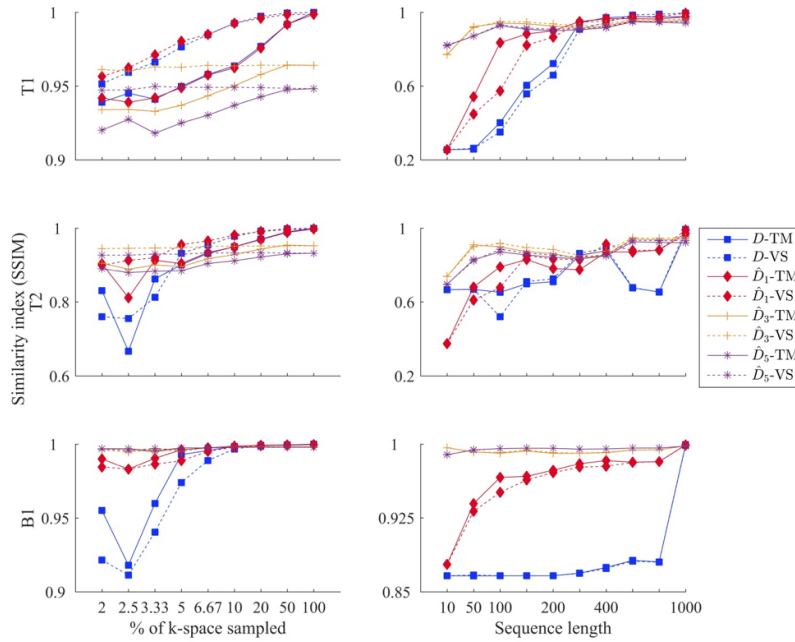


Fig. 4. Acceleration in space and time. The left column displays the SSIM for each of the dictionaries and two reconstruction methods: template matching (TM) and view-sharing (VS) for different levels of k-space sampling. The right column shows the estimated SSIM for increasing sequence length and an acceleration factor $R=5$ (20% of k-space).

data for kernel sizes larger than $P = 3 \times 3 \times 3$. In fact, the amount of training observations required and the corresponding size of the dictionary in terms of space, time, and clusters, leads to two important discussion points: 1) using clustering enables higher acceleration, at the expense of disregarding parameter combinations that are not present in the training set (e.g. pathology); and 2) adding spatial information increases the dimensionality of the dictionary, requiring approaches that can effectively deal with matching in high dimensional spaces.

5 Conclusions

We propose a method to create clustered MRF dictionaries and show the added benefit of combining it with a view-sharing strategy to enable both accelerated acquisitions by undersampling, and accelerated reconstructions through dictionary compression. Further investigation of data-driven approaches could pave the way towards tissue and disease specific dictionaries in clinical settings.

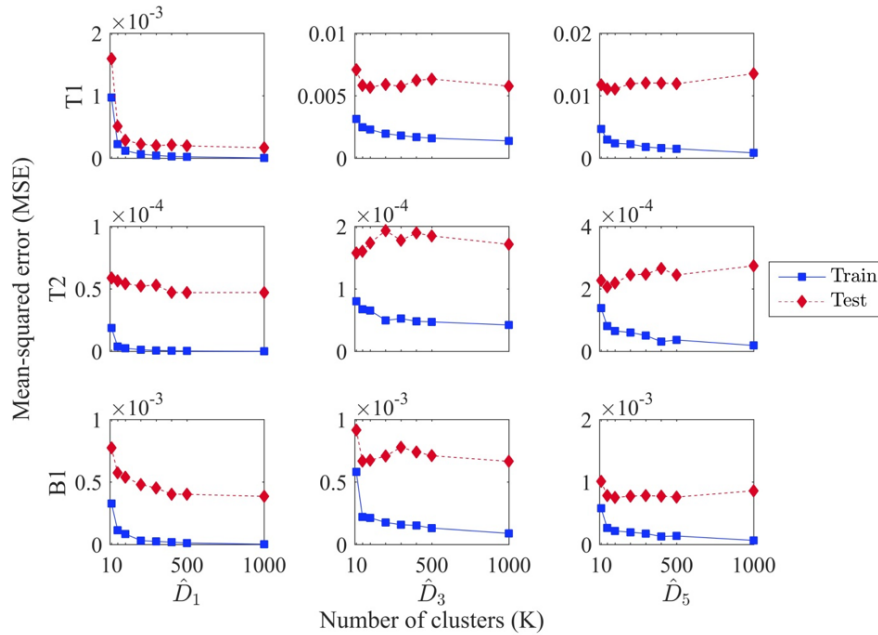


Fig. 5. Training and testing error for different cluster sizes K from the fully sampled reference dataset. For \hat{D}_1 both the training and testing error reduce with an increasing number of clusters, while testing errors for \hat{D}_3 and \hat{D}_5 do not change significantly with increasing clusters.

References

1. Buonincontri, G., Sawiak, S.: Three-dimensional MR fingerprinting with simultaneous B1 estimation. *Magnetic Resonance in Medicine* 00, 1–9 (2015)
2. Gómez, P.A., Ulas, C., Sperl, J.I., Sprenger, T., Molina-Romero, M., Menzel, M.I., Menze, B.H.: Learning a spatiotemporal dictionary for magnetic resonance fingerprinting with compressed sensing. *MICCAI Patch-MI Workshop* 9467, 112–119 (2015)
3. Jiang, Y., Ma, D., Seiberlich, N., Gulani, V., Griswold, M.A.: MR Fingerprinting Using Fast Imaging with Steady State Precession (FISP) with Spiral Readout. *MRM* (2014)
4. Ma, D., Gulani, V., Seiberlich, N., Liu, K., Sunshine, J.L., Duerk, J.L., Griswold, M.A.: Magnetic resonance fingerprinting. *Nature* 495, 187–192 (2013)
5. Wang, Z., Bovik, A.C., Sheikh, H.R., Simoncelli, E.P.: Image quality assessment: From error visibility to structural similarity. *IEEE Transactions on Image Processing* 13, 600–612 (2004)